

Low-Profile, Multi-Element, Miniaturized Monopole Antenna

Wonbin Hong, *Student Member, IEEE*, and Kamal Sarabandi, *Fellow, IEEE*

Abstract—A low-profile, electrically small antenna with omnidirectional vertically polarized radiation similar to a short monopole antenna is presented. The antenna features less than $\lambda/40$ dimension in height and $\lambda/10$ or smaller in lateral dimension. The antenna is matched to a $50\ \Omega$ coaxial line without the need for external matching. The geometry of the antenna is derived from a quarter-wave transmission line resonator fed at an appropriate location to maximize current through the short-circuited end. To improve radiation from the vertical short-circuited pin, the geometry is further modified through superposition of additional resonators placed in a parallel arrangement. The lateral dimension of the antenna is miniaturized by meandering and turning the microstrip lines into form of a multi-arm spiral. The meandering between the short-circuited end and the feed point also facilitates the impedance matching. Through this technique, spurious horizontally polarized radiation is also minimized and a radiation pattern similar to a short dipole is achieved. The antenna is designed, fabricated and measured. Parametric studies are performed to explore further size reduction and performance improvements. Based on the studies, a dual-band antenna with enhanced gain is realized. The measurements verify that the proposed fabricated antennas feature excellent impedance match, omnidirectional radiation in the horizontal plane and low levels of cross-polarization.

Index Terms—Dual-band antennas, electrically small antennas, monopole antennas, omnidirectional antennas.

I. INTRODUCTION

THE half-wave dipole antenna is perhaps one of the most fundamental and commonly used antennas ever since the discovery of electromagnetic wave radiation. From the early stages to present, the dipole antenna and its variations have been extensively used in the field of wireless communication for its simple geometry and reliability. In addition when the antenna is vertically mounted, the dipole antenna features an omnidirectional radiation pattern, making it useful for terrestrial applications, non-line-of sight conditions, and situations where transceiver modules are often deployed randomly. For near ground wave propagation applications where both the transmit and receive antennas are placed near the surface of the earth, it is shown that propagation path loss for vertically oriented antennas is by many magnitude lower than any other antenna orientation configuration. Monopoles that emulate virtually identical performance behaviors as that of a dipole antenna are often used at lower frequencies. For air or ground vehicle applications it

is highly desirable to use low-profile antennas that can produce vertical polarization with omnidirectional radiation pattern. Also applications such as network of unattended ground sensors, low-profile antennas are highly desired. As wireless communication devices continue to evolve, the large dimension of the antenna is frequently problematic. Therefore it is imperative to further investigate methods of realizing extremely short monopole antennas with very small lateral dimensions. This will allow integration of such antennas with the wireless device package or platform.

A variety of space filling compression techniques have been studied to reduce the vertical profile of monopole antennas [1]–[3]. The dimension of a wire monopole antenna is greatly reduced by folding the monopole antenna geometry through several iterations. In [4], metallic paths patterned after Peano and Hilbert curves are used to greatly reduce the vertical profile of monopole antennas. The Peano-curve top-loaded monopole features a vertical height of approximately $\lambda/12$ while featuring excellent monopole radiation pattern. In addition, a meandered monopole antenna is further modified by extending a conductor line for the end of a rectangular meander monopole to achieve a dual-band operation [5]. In [6], [7], various fractal antennas are further investigated and the resonant properties, bandwidth, and impedance matching of compressed omnidirectional antennas are reported.

The vertical height of a monopole antenna can also be reduced through antenna loading techniques. In [8], the antenna is loaded with a dielectric cylinder and a dual-band behavior is realized. A monopole antenna is inductively loaded and its electrical characteristic is studied [9], [10]. In [11]–[16], a low-profile, omnidirectional antenna is reported by capacitively loading a monopole antenna with modified disks. The heights of the proposed antennas are in the range of $\lambda/10$. In addition, these antennas feature excellent operational bandwidth. However, the lateral dimension of the antennas are comparable to wavelength. Nonetheless, the impact of the Goubau antenna [16] is significant in the antenna community due to the fact that it closely approaches Chu's fundamental limit. However, because of its complex geometry, the Goubau antenna is difficult to be analyzed using conventional methods. In [17], the Goubau antenna is thoroughly analyzed using full-wave simulations. Recently, artificial electromagnetic materials such as electromagnetic band-gap (EBG) structures have been incorporated with conventional wire antennas to feature a low-profile antenna that behave equivalent to a vertical monopole antenna [18].

In this paper, a low-profile antenna with omnidirectional vertically polarized radiation similar to that of a traditional monopole antenna is proposed and presented using a different approach. The proposed antenna is realized by modifying the

Manuscript received March 26, 2008; revised August 11, 2008. Current version published March 04, 2009.

Authors are with the Radiation Laboratory, Department of Electrical Engineering and Computer Science, The University of Michigan, Ann Arbor, MI 48109-2122 USA (e-mail: wonbin@umich.edu).

Digital Object Identifier 10.1109/TAP.2008.2009731

geometry of a quarter-wave microstrip type resonator to emulate an electrically small antenna with a very small vertical profile. The concept is based on superposition of multiple quarter-wave segments that are meandered and spiraled around to virtually negate the radiation from horizontal currents above the ground plane. As a result, the antenna features a vertically polarized radiation in the horizontal plane. The design and miniaturization method for the antenna is presented in Section II. Simulation and measurement results are also shown and discussed. The antenna is further modified and parametric studies are done in Section III. In Section IV, a dual-band multi-element monopole antenna is designed and its measurement results are presented and discussed.

II. THE MINIATURIZED MULTI-ELEMENT MONOPOLE ANTENNA

Radiation powers from short monopole antennas are proportional to the currents induced on them. In practice the level of induced current is limited by the impedance mismatch between the transmission line and the very small radiation resistance of such radiating structures. External matching networks based on lumped elements are lossy which render a rather poor radiation efficiency. One approach to increase the induced electric current on a short segment of a vertical wire above a ground plane is to use the vertical wire as part of a resonant structure. The smallest resonant structure can be formed from a quarter-wavelength segment of a transmission line short-circuited at one end and open-circuited at the other end (i.e., monopole). Consider a microstrip line resonator formed by a strip above the ground plane and short-circuited by a small vertical wire. This resonator can be fed from the center as shown in Fig. 1(a). Impedance matching of this quarter-wavelength resonator (monopole) is facilitated by adjusting the feed position along the resonator and choosing parameters l_{open} , the open-circuited segment and l_{short} , the short-circuited segment. It is expected that the current flowing on the microstrip itself does not contribute to the total radiated field due to cancellation of the far-field by its image in the ground plane. The directions of the currents at the feed point and on the short-circuited vertical wire are opposite of each other; however, the magnitude of current at the short-circuited wire can be significantly higher from which the net radiation emanates. The electric current flowing on the vertical element of the antenna is responsible for the vertically polarized radiation. If the horizontal electric current can be effectively eliminated we can achieve a completely vertically polarized radiation ignoring the lateral electrical dimension for the time being. Cancellation can be done by adding another monopole element while sharing the same feed as seen in Fig. 1(b). The cancellation of the horizontal electric current is achieved by introducing another set of electric current that is in the opposite direction in the horizontal plane of the antenna with the original electric current at electromagnetic resonance. In contrast, the vertical electric currents flowing on the short-circuited pins of each elements is in phase and as a result, behaves as the radiating elements of the antenna. Thus, the two-element monopole antenna behaves as a small vertically polarized antenna. To achieve omnidirectional radiation patterns in the horizontal plane of the antenna while maintaining low levels of cross-polarization levels, it is important for

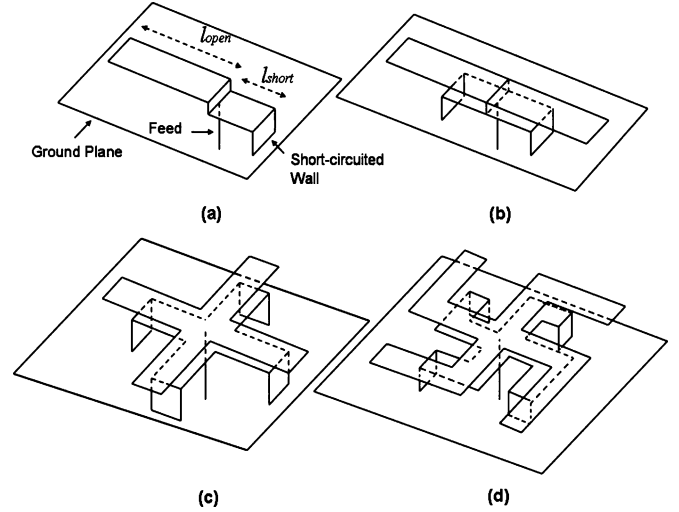


Fig. 1. Design process of the miniaturized multi-element monopole antenna.

the antenna to be electrically small and symmetric. Additional monopole elements are added in similar ways to negate the horizontal currents. The increased number of short-circuited pins provides increased number of radiators and improves the mechanical stability of the multi-element monopole antenna. Parameters l_{open} and l_{short} must be modified to accommodate for the changes in impedance caused by the additional monopole elements. The topology of the four-element monopole antenna is presented in Fig. 1(c).

The proposed topology of the multi-element monopole antenna enables the height of a traditional monopole antenna to be greatly reduced. However, as the height of the multi-element monopole antenna reduces, the lateral dimension increases. The miniaturization of the multi-element monopole antenna is achieved by folding the open-circuited segments of the antenna in a spiral-shaped geometry so the cancellation of horizontal electric currents on the elements is maintained. To achieve miniaturization, the short-circuited segments of the antenna can also be meandered and placed slightly below the spiral layer. A sketch of a miniaturized multi-element monopole antenna is visualized in Fig. 1(d). The overall length of each quarter-wavelength segment must be adjusted using a full-wave approach to take the effects of near field mutual couplings into account.

The miniaturized multi-element monopole antenna is designed using Ansoft's HFSS. The topology of the simulated antenna is presented in Fig. 2. Parameters are optimized to achieve operation around 460 MHz with lateral dimensions less than $\lambda/10$ and the height to be around $\lambda/30$. The open-circuited elements and the short-circuited elements are designed on two separate vertical layers with 1 mm spacing for enhanced space conservation and compactness. The open-circuited elements are folded in a spiral-like fashion and minimized to $W_c \times L_c = 56 \text{ mm} \times 56 \text{ mm}$ in lateral dimension. The total length of the open-circuited element (l_{open}) is 117 mm. The miniaturized open-circuited elements are fed by a single wire feed. The meandered short-circuited elements are designed to be placed 1 mm beneath the miniaturized open-circuited elements. The elements in both layers are electrically connected by four

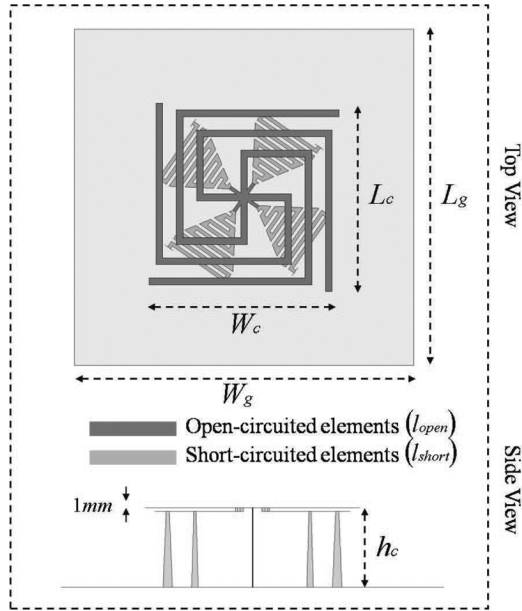


Fig. 2. Topology of the miniaturized multi-element monopole antenna.

vertical pillars with a height of 1 mm. The short-circuited pins are connected to each end of the four short-circuited elements respectively. The total length from the vertical pillar to the short-circuited pin (l_{short}) is 94.6 mm. Impedance matching of the miniaturized multi-element monopole is achieved by adjusting the length of the meandered short-circuited elements. The antenna is then fabricated on a 0.3 mm thick copper sheet. The open-circuited and short-circuited elements on each vertical layers are milled separately and soldered together. A 1 mm thick dielectric spacer is placed between the two layers to minimize fabrication and simulation discrepancies. The short-circuited pins are milled to be 20 mm in height (h_c) and then soldered to each ends of the meandered short-circuited elements respectively. The short-circuited pins are then soldered to a $W_g \times L_g = 100 \text{ mm} \times 100 \text{ mm}$ copper ground plane. The final height of the fabricated antenna is 21.3 mm.

Fig. 3 shows the simulated and measured input reflection coefficient of the proposed antenna. The fabricated antenna features 3% 2:1 VSWR bandwidth. The slight discrepancy between the simulated and measured responses can be attributed to alignment errors during the fabrication process. The radiation patterns of the miniaturized multi-element monopole antenna is measured in the anechoic chamber of the University of Michigan at the resonant frequency of 460 MHz. Fig. 4 shows the E- and H- Plane, co- and cross-polarized patterns of the antenna. The measured antenna features omnidirectional radiation pattern in the H-Plane, similar to a monopole. In addition, a null is observed at $\Theta = 0^\circ$ in the E-Plane. Cross-polarization levels in both planes are mainly caused by the close proximity of the feed network cable and the small ground plane size. This can be confirmed with simulated radiations patterns of the featured antenna on an infinite ground plane as presented in Fig. 5. The gain of the miniaturized multi-element monopole antenna is measured in the anechoic chamber using a dipole antenna with a known gain. The gain is measured to

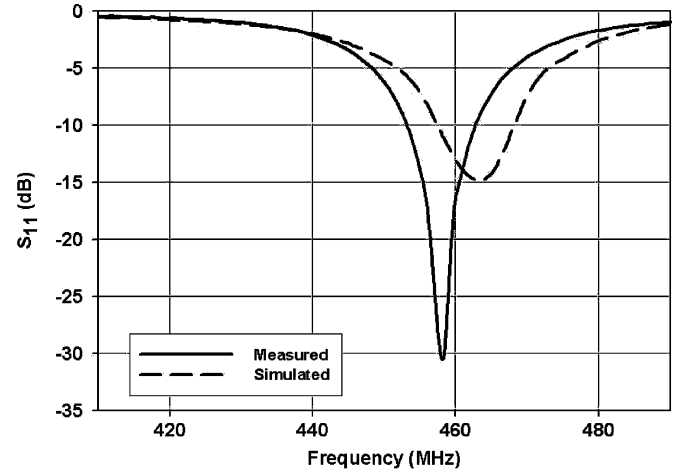


Fig. 3. Measured and simulated S_{11} response of the miniaturized multi-element monopole antenna.

be -4.1 dBi. The directivity is calculated to be 1.0 dBi. For such electrically small ground plane dimension ($\lambda/7 \times \lambda/7$) the effect of the edge currents on the ground plane becomes significant to the radiation pattern, directivity, and gain of the proposed antenna. Strong levels of edge currents result in the rise of cross-polarization levels, increased ohmic loss leading to degradation of directivity and gain. In addition, the low gain suggest that relatively high levels of currents on the open-circuited and short-circuited elements may be causing ohmic loss. Therefore it is important to further investigate the topology of the antenna and the effects of the ground plane.

III. THE MODIFIED MULTI-ELEMENT MONOPOLE ANTENNA

A. Antenna Design

Now that the functionality of the proposed miniaturized multi-element monopole antenna has been established, additional modifications are made to the antenna design to further improve its performance. To reduce fabrication errors and improve rigidity, the antenna is newly designed on a dielectric substrate. As discussed in the previous section, the input impedance matching of the antenna is achieved by adjusting the length of the meandered element of the antenna. However, such modification is rather complex, requiring the topology of the antenna to be redesigned and fabricated. Therefore, impedance matching is difficult to achieve through simple tuning of the antenna topology. It has been shown that the length of a slot antenna can significantly be reduced by inserting short-circuited narrow slot-lines along the radiating segment of a slot antenna [19]. Basically, the short-circuited narrow slot-lines behave as series inductive elements. Due to the insertion of series inductive elements, the electric current on the ground plane then transverses a longer path. As result the resonant frequency decreases. The meandered short-circuited elements of the miniaturized multi-element monopole antenna are replaced with a similar geometry. The meandered short-circuited elements are first straightened. Then a pair of 0.5 mm wide open-circuited microstrip lines are inserted along the straightened elements. The insertion of narrow open-circuited microstrip lines introduces shunt capacitance stubs

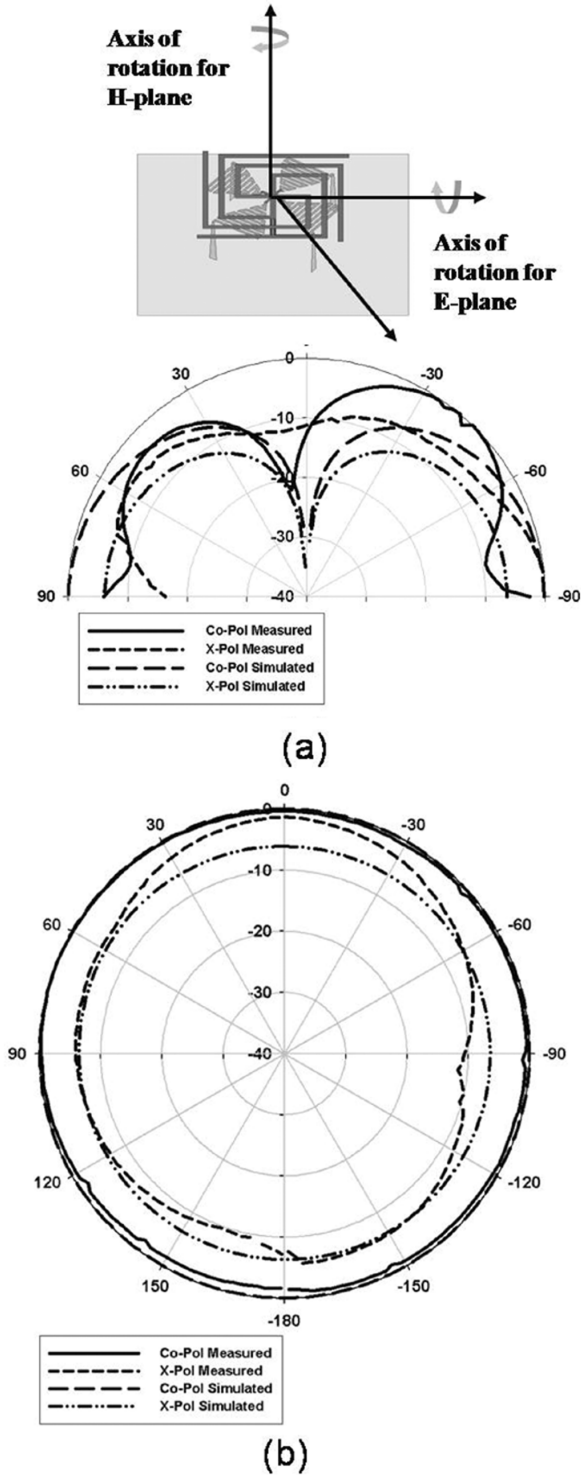


Fig. 4. Measured and simulated radiation pattern of the miniaturized multi-element monopole antenna. (a) E-Plane. (b) H-Plane.

which have a similar size reduction effect. Thus, the physical lengths of the straightened short-circuited elements are reduced. Impedance matching is obtained by simply adjusting the location ($c_a = 3.5$ mm) and lengths ($l_a = 4.2$ mm) of the inserted narrow microstrip lines. The right angle edges of the spiral-shaped open-circuited elements are replaced with curved edges. The final lengths of the open-circuited elements $l_{open,m}$

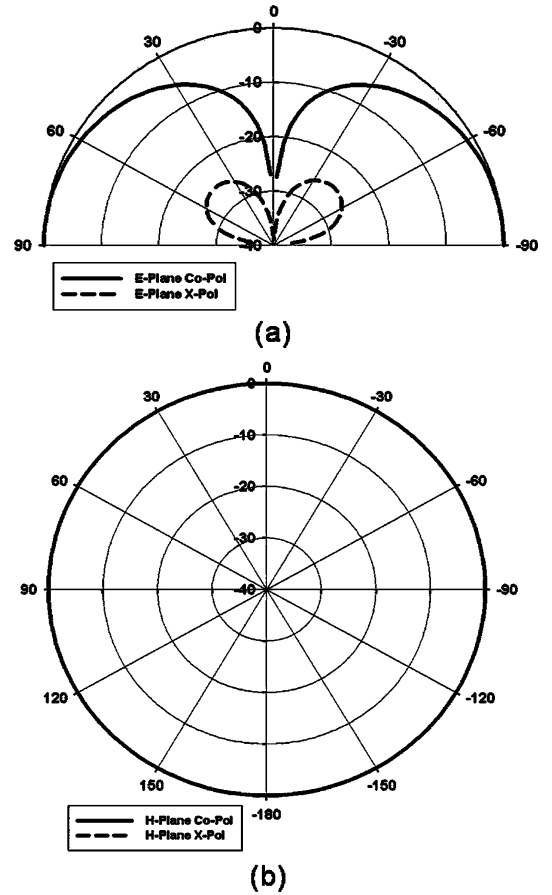


Fig. 5. Simulated radiation pattern of the miniaturized multi-element monopole antenna on an infinite ground plane. (a) E-Plane. (b) H-Plane.

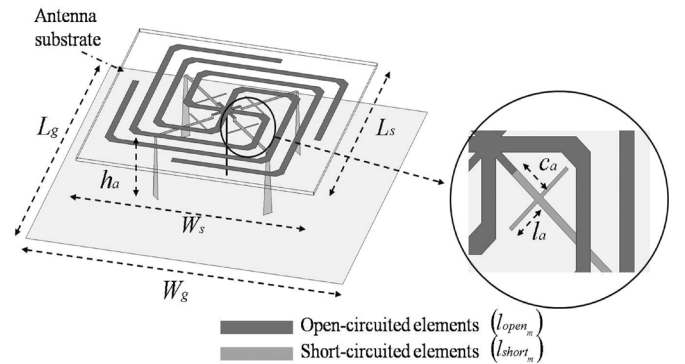


Fig. 6. Topology of the modified multi-element monopole antenna. The inserted open-circuited microstrip is shown in the right.

and short-circuited elements $l_{short,m}$ are 144 mm and 20 mm respectively. The modified geometry is shown in Fig. 6.

B. Fabrication and Measurement

The modified antenna is simulated and then fabricated using a $W_s \times L_s = 75$ mm \times 75 mm Rogers5880 with thickness of 1 mm, dielectric constant of $\epsilon_a = 2.2$, and loss tangent of $\tan \delta_a = 0.0009$. The two layers of the antenna geometry are etched on the top and bottom side of the dielectric substrate. The two layers are then connected through via holes. The short-

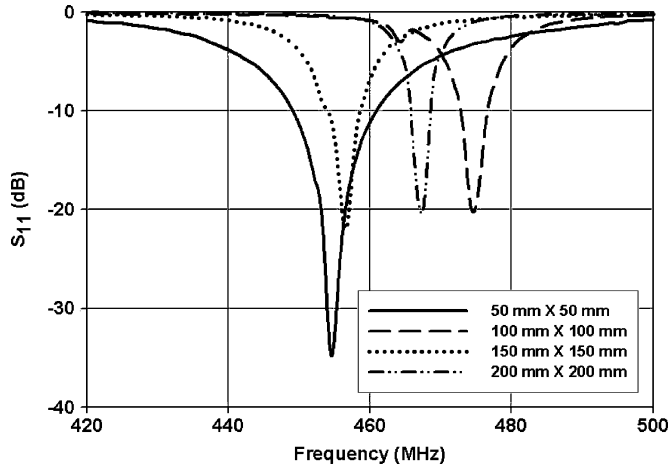


Fig. 7. Measured S_{11} response of the modified multi-element monopole antenna as a function of ground plane dimension.

circuited pins are connected to each end of the four short-circuited elements. The integrated antenna structure is then soldered on to a $W_g \times L_g = 50 \text{ mm} \times 50 \text{ mm}$ ground plane. The antenna is fed from the center using a coaxial feed. The antenna height (h_a) is set to 20 mm. The return loss of the fabricated modified multi-element monopole antenna is presented in Fig. 7. The antenna displays good impedance matching and 3.5% 2:1 VSWR bandwidth. The far-field co-polarized ($|E_\theta|^2$) and ($|E_\phi|^2$) radiation patterns of the antennas are presented in Figs. 8(a) and 9(a) respectively. The measured pattern indicates the radiation pattern of the antenna remains similar to that of the original miniaturized multi-element monopole antenna after the modification. As expected due to the small ground plane dimension, the modified antenna features relatively high levels of cross-polarization levels. The gain of the modified multi-element monopole antenna is measured to be -3.3 dBi , indicating the improved geometry enhances the radiation efficiency of the antenna compared to the original miniaturized multi-element monopole antenna.

C. Parametric Studies

The dimension of the ground plane is increased to examine how the parameter affects the performance of the modified multi-element monopole antenna. The antenna is subsequently fabricated and measured on four different ground planes with increasing dimension. No additional modifications to the topology of the antenna is performed as the dimension of the ground plane changes. The measured input reflection responses of the antennas are presented in Fig. 7. It is observed that the antenna remains to be well matched as the size of the ground plane varies. The shift in resonant frequency can mostly be attributed to the radiating ground plane currents which slightly modify the radiation of the antenna. The measured 2:1 VSWR bandwidths, gains, and the calculated directivities of the antennas associated with different ground plane sizes are listed in Table I. The measured and simulated radiation patterns in Figs. 8 and 9 show as the ground plane dimension increases, cross-polarization levels decrease accordingly. As expected the gain increases as a result. It can be seen from Table I that

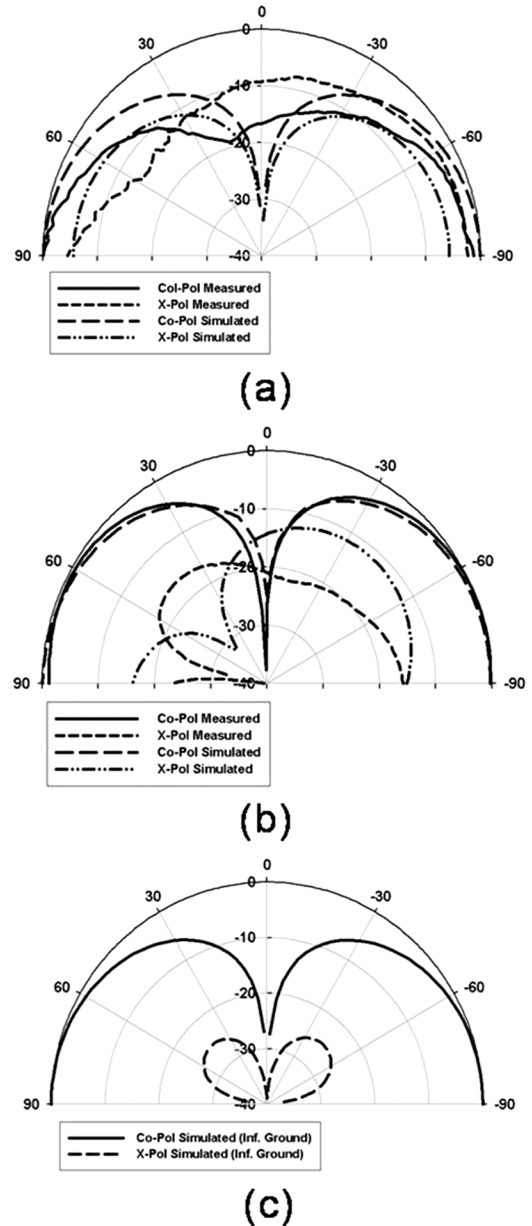


Fig. 8. Measured and simulated E-Plane radiation pattern of the modified multi-element monopole antenna as a function of ground plane dimension. (a) $W_g \times L_g = 50 \text{ mm} \times 50 \text{ mm}$. (b) $W_g \times L_g = 200 \text{ mm} \times 200 \text{ mm}$. (c) Infinite ground plane.

the gain of the modified multi-element monopole antenna is enhanced by more than 5 dB as the dimension of the ground plane increases to $200 \text{ mm} \times 200 \text{ mm}$.

It is important to study the effect of the height of the modified multi-element monopole antenna on its gain and bandwidth. The height of the antenna from the metal ground plane is incremented from $h_a = 10 \text{ mm}$ to $h_a = 30 \text{ mm}$ by adjusting the height of the short-circuited pins. The modified antennas are then fabricated on a $W_g \times L_g = 200 \text{ mm} \times 200 \text{ mm}$ ground plane. Fig. 10 shows the measured input reflection response of the antennas with different heights. The measured 2:1 VSWR bandwidths and gains are listed in Table II. The measured results indicates that the height of the antenna can be further reduced to less than $\lambda/25$ without suffering severe gain degradation which

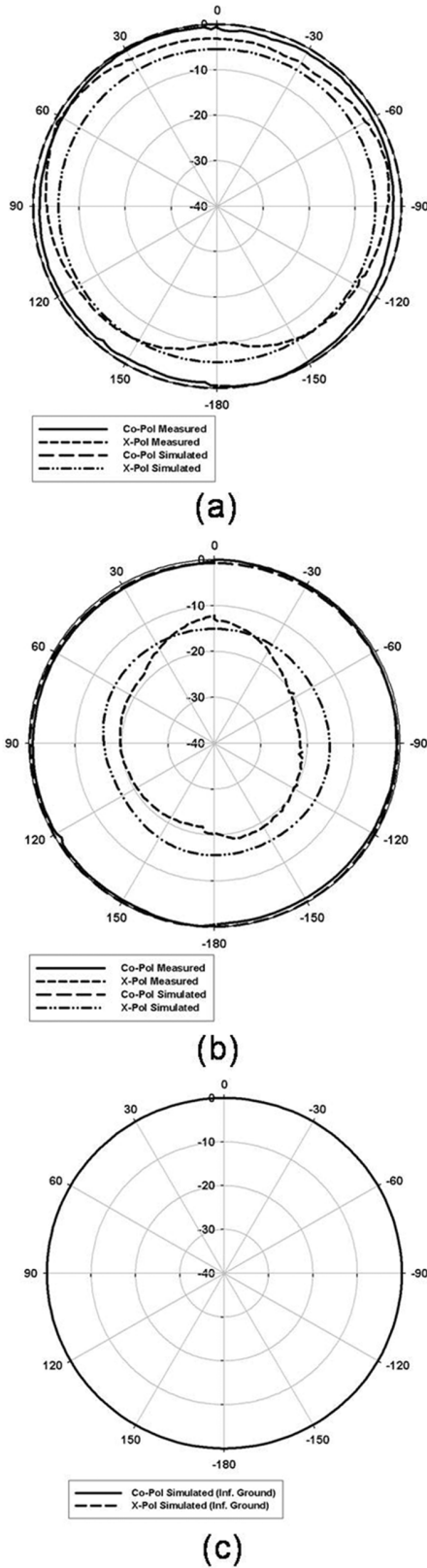


Fig. 9. Measured and simulated H-Plane radiation pattern of the modified multi-element monopole antenna as a function of ground plane dimension. (a) $W_g \times L_g = 50 \text{ mm} \times 50 \text{ mm}$. (b) $W_g \times L_g = 200 \text{ mm} \times 200 \text{ mm}$. (c) Infinite ground plane.

is important for low-profile, vertically-polarized antennas. The fabricated antennas are shown in Fig. 16.

IV. THE DUAL-BAND MULTI-ELEMENT MONOPOLE ANTENNA

A. Antenna Design

It has been shown in the previous section that the gain of the modified multi-element monopole antenna can greatly be enhanced by increasing the size of the ground plane. For small antennas, due to ohmic losses the bandwidth is found to be inversely proportional to the gain. Therefore in this section, additional methods are investigated and discussed to further increase the bandwidth while maintaining the gain of the proposed antenna.

The fundamental resonance of the miniaturized multi-element monopole antenna is determined by the overall length of the antenna arms. As mentioned earlier, the length of the each arm of the antenna is designed to be of identical length to ensure an electrical symmetry of the antenna structure. Therefore each arm of the antenna features an identical electromagnetic resonance. Adjusting the length of each arm to be of different lengths is found to be ineffective in achieving multi-resonance behavior. Instead, a single resonance which is approximately the average of the combined resonances of each different arms is observed. In addition, transmission zeros limits the multiple resonances from being effectively combined for bandwidth enhancement. Thus, a parasitic coupling approach is used to further improve the bandwidth of the proposed antenna. The dual-band miniaturized multi-element monopole antenna is designed by adding an additional parasitic antenna topology on top of the original modified multi-element monopole antenna structure. Fig. 11 shows the geometry of the proposed dual-band antenna. The driven and parasitic antenna-elements of the proposed antenna are separated by spacing d , which is adjusted by modifying the vertical heights (h_p) of the short-circuited pins of the parasitic antenna-element. The coaxial feed is connected to the driven antenna-element. The driven and parasitic antenna-elements are presented in Figs. 12 and 13 respectively. For the driven antenna element, the open-circuited element and the short-circuited element is designed to be on the top and bottom side of the driven antenna-element substrate respectively, similar to the original single resonance miniaturized multi-element monopole antenna. However, it should be noted that for the parasitic antenna-element, the configuration of the open-circuited element and the short-circuited element is reversed. The open-circuited element for the parasitic antenna-element is placed on the bottom side of the parasitic antenna-element substrate. Such modification is made to ensure the two antenna-elements are electrically coupled at similar locations. By doing so, the electric fields in both antenna-elements will be in phase and therefore the far field radiation is enhanced. Impedance matching is achieved by adjusting the lengths and locations of the inserted 0.5 mm wide open-circuited microstrip-lines for each respective antenna-elements. The final design parameters of the dual-band multi-element monopole antenna are provided in Table III.

B. Fabrication and Measurement

The dual-band multi-element monopole antenna follows similar fabrication procedure as its single-resonance predecessor. The antenna is simulated using HFSS. Then, both driven and

TABLE I
MEASURED BANDWIDTH AND GAIN AND COMPUTED DIRECTIVITY AS A FUNCTION OF GROUND PLANE DIMENSION. THE ANTENNA HEIGHT (h_a) IS 20 MM

2:1 VSWR (%)	Measured Gain (dBi)	Directivity (dBi)	$W_g \times L_g$ (mm)
3.5	-3.3	1.0	50 × 50
1.6	-1.1	1.1	100 × 100
1.8	0.4	2.0	150 × 150
0.6	1.6	2.8	200 × 200

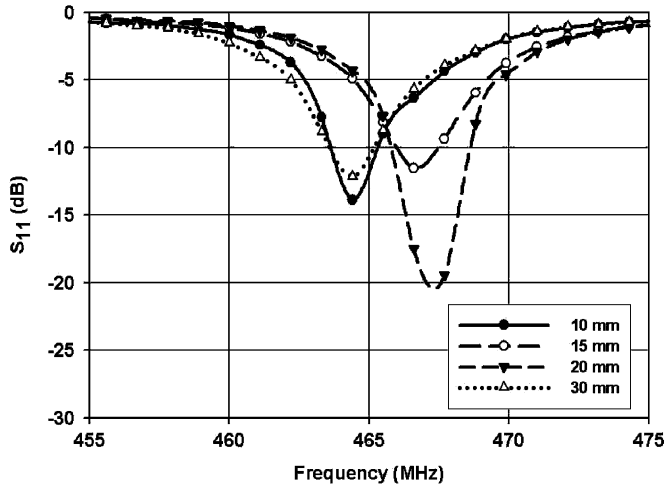


Fig. 10. Measured S_{11} response of the modified multi-element monopole antenna as a function of antenna height h_a .

TABLE II
MEASURED BANDWIDTH AND GAIN AS A FUNCTION OF ANTENNA HEIGHT. THE GROUND PLANE DIMENSION IS $W_g \times L_g = 200$ mm × 200 mm

2:1 VSWR (%)	Measured Gain (dBi)	Antenna height h_a (mm)
0.4	-3.1	10 ($\lambda/40$)
0.5	1.0	15 ($\lambda/27$)
0.6	1.6	20 ($\lambda/20$)
0.5	1.9	30 ($\lambda/13$)

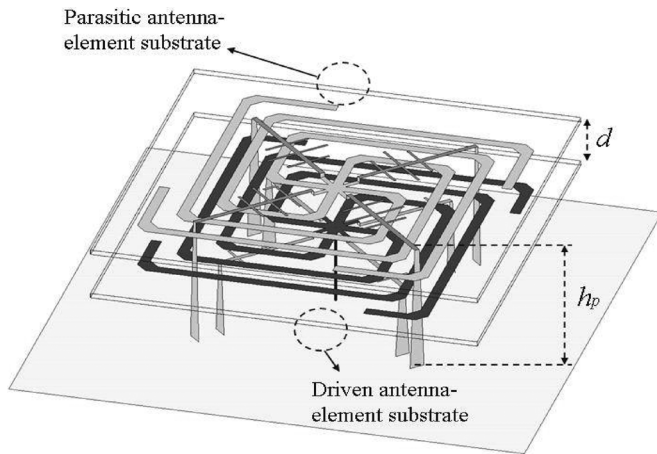


Fig. 11. Topology of the dual-band multi-element monopole antenna.

parasitic antenna-elements are etched using identical substrates. The short-circuited pins are then connected to their respective

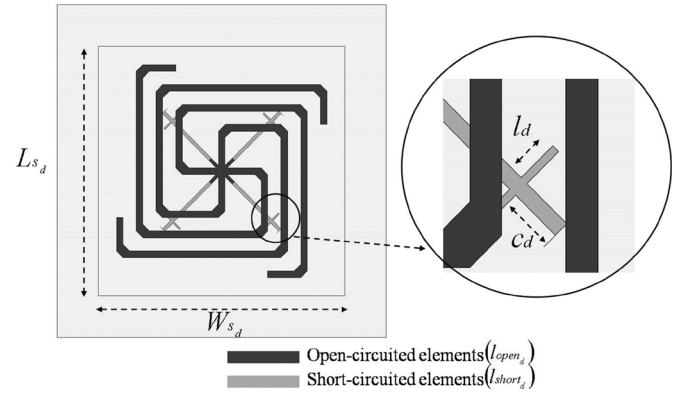


Fig. 12. Topology of the driven antenna-element of the dual-band multi-element monopole antenna. The inserted open-circuited microstrip is shown in the right.

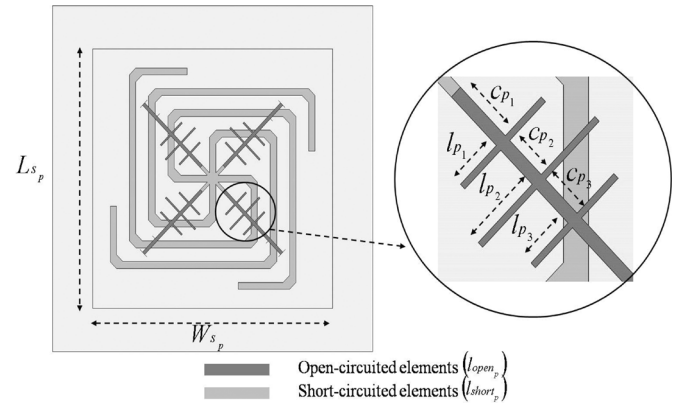


Fig. 13. Topology of the parasitic antenna-element of the dual-band multi-element monopole antenna. The inserted open-circuited microstrip is shown in the right.

TABLE III
DESIGN PARAMETERS OF THE DUAL-BAND MULTI-ELEMENT MONOPOLE ANTENNA (MM). THE GROUND PLANE DIMENSION IS $W_g \times L_g = 200$ mm × 200 mm

l_{open_d}	l_{short_d}	l_d	c_d	W_{s_d}	L_{s_d}	l_{open_p}	l_{short_p}
118	20	2.8	2.5	75	75	126	25.5
l_{p_1}	l_{p_2}	l_{p_3}	c_{p_1}	c_{p_2}	c_{p_3}	W_{s_p}	L_{s_p}
4	6	4.1	3.5	2.5	2.5	75	75

locations. Small holes are drilled through both of the antenna-element substrates for the short-circuited pins of the parasitic antenna-element. A dielectric spacer is placed between the two antenna-element substrates while the short-circuited pins are

TABLE IV
MEASURED BANDWIDTH AND GAIN AS A FUNCTION OF SPACING d

	Resonant Frequency (MHz)	2:1 VSWR (%)	Measured Gain (dBi)	Antenna height h_p (mm)	d (mm)
<i>Dual-band</i>	453	0.6	2.0	28	7
	465	0.7	2.2	28	7
<i>Wideband</i>	460	2.2	2.0	31	10

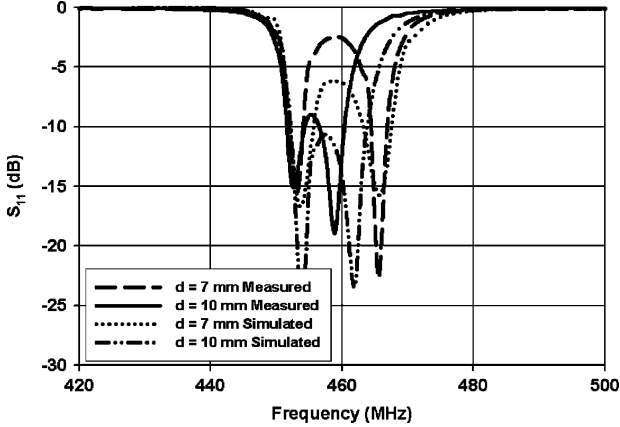


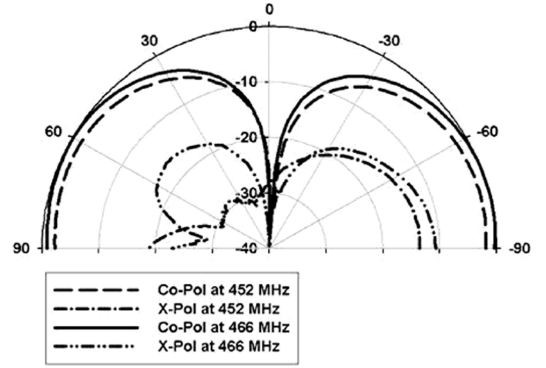
Fig. 14. Measured and simulated S_{11} response of the dual-band multi-element monopole antenna as a function of spacing d .

connected to the substrates. The assembled antenna topology is then connected to a $W_g \times L_g = 200 \text{ mm} \times 200 \text{ mm}$ ground plane. Finally, a coaxial cable is connected to the driven antenna-element. The measured and simulated return losses of the dual-band antenna is presented in Fig. 14. As can be observed from the figure, by adjusting d , the two resonances of the antenna can be controlled to split or merge with one another. The far-field co-polarized ($|E_\theta|^2$) and ($|E_\phi|^2$) radiation patterns of the antenna are presented in Fig. 15. It can be observed that the radiation pattern remains similar to a traditional monopole antenna throughout the operating frequency band. In addition, the added parasitic antenna-element does not appear to cause increased levels of cross-polarized radiations. The measured 2:1 VSWR bandwidths and gains of the dual-band multi-element antenna with different spacing d are presented in Table IV.

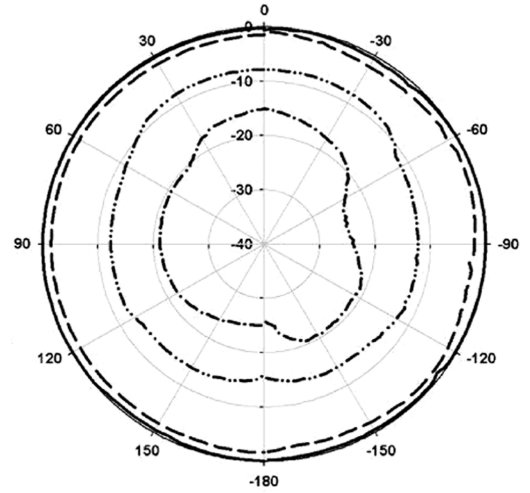
Compared to the original multi-element monopole antenna with identical ground plane dimension, the dual-band multi-element monopole antenna features enhanced bandwidth without gain degradation. By controlling the spacing d , the wideband response is measured to have more than twice the 2:1 VSWR bandwidth of the individual bands of the dual-band response. The addition of a parasitic antenna-elements results in increasing the overall height of the antenna by 50%. However, it has been shown that the height can be further reduced without significant performance tradeoff.

V. CONCLUSION

An antenna miniaturization approach is proposed and discussed. Using this approach, an electrically small antenna is designed, emulated, and measured. The featured multi-element monopole antenna displays similar radiation behavior as that of a traditional vertical monopole antenna while having a vertical

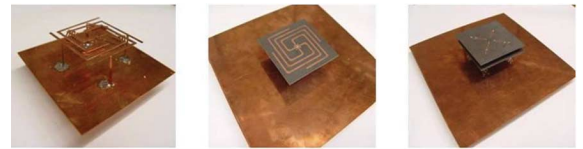


(a)



(b)

Fig. 15. Measured radiation pattern of the dual-band multi-element monopole antenna. (a) E-Plane. (b) H-Plane. ($d = 10 \text{ mm}$).



(a)

(b)

(c)

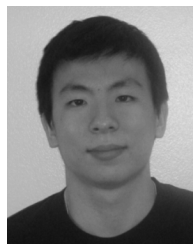
Fig. 16. Photograph of the fabricated antennas. (a) Miniaturized multi-element monopole antenna. (b) Modified multi-element monopole antenna. (c) Dual-band/wideband multi-element monopole antenna.

profile as low as $\lambda/40$. The lateral dimension of the multi-element monopole antenna is significantly reduced by folding the open-circuited elements in a spiral-shaped geometry. Parametric studies are performed to investigate further antenna miniaturization and performance improvements. The measured multi-element monopole antenna displays omnidirectional

pattern in the horizontal plane of the antenna and low levels of cross-polarized radiations. In addition, the proposed antenna is modified to feature enhanced bandwidth and excellent gain.

REFERENCES

- [1] J. Rashed and C. T. Tai, "A new class of resonant antennas," *IEEE Trans. Antennas Propag.*, vol. 39, pp. 1498–1430, Sept. 1991.
- [2] C. Puente-Baliarda, J. Romeu, and A. Cardama, "The Koch monopole: A small fractal antenna," *IEEE Trans. Antennas Propag.*, vol. 48, pp. 1773–1781, Nov. 2000.
- [3] C. Puente-Baliarda, J. Romeu, R. Pous, and A. Cardama, "On the behavior of the Sierpinski multiband fractal antenna," *IEEE Trans. Antennas Propag.*, vol. 46, pp. 517–528, Apr. 1998.
- [4] J. McVay and A. Hoorfar, "Miniaturization of top-loaded monopole antennas using Peano-curves," in *Proc. IEEE Radio and Wireless Symp.*, Jan. 9–11, 2007, pp. 253–256.
- [5] H. Chen, W. Chen, Y. Cheng, and Y. Lin, "Dualband monopole antenna," in *IEEE Int. Symp. on Antennas Propag.*, June 22–27, 2003, vol. 3, pp. 48–51.
- [6] S. R. Best, "A comparison of the resonant properties of small space-filling fractal antennas," *IEEE Antennas Wireless Propag. Lett.*, vol. 2, pp. 197–199, 2003.
- [7] J. Zhu, A. Hoorfar, and N. Engehta, "Bandwidth, cross-polarization, and feed-point characteristics of matched hilbert antennas," *IEEE Antennas Wireless Propag. Lett.*, vol. 2, pp. 2–5, 2003.
- [8] Y. F. Lin, C. H. Lin, and P. S. Hall, "A miniature dielectric loaded monopole antenna for 2.4/5 GHz WLAN applications," *IEEE Microw. Wireless Compon. Lett.*, vol. 16, pp. 591–593, Nov. 2006.
- [9] A. Pomerleau and M. Fournier, "Inductively loaded monopole antenna," in *IEEE Int. Symp. on Antennas Propag.*, Dec. 1972, vol. 10, pp. 81–84.
- [10] C. Harrison, Jr., "Monopole with inductive loading," *IEEE Trans. Antennas Propag.*, vol. 11, pp. 394–400, Jul. 1963.
- [11] J. McLean, H. Foltz, and G. Crook, "Broadband, robust, low profile monopole incorporating top loading, dielectric loading, and a distributed capacitive feed mechanism," in *Proc. IEEE Int. Symp. on Antennas Propag.*, Jul. 11–16, 1999, vol. 3, pp. 1562–1565.
- [12] S. Tokumaru, "Multiplates: Low profile antennas," in *IEEE Int. Symp. on Antennas Propag.*, Oct. 1976, vol. 14, pp. 379–382.
- [13] N. Herscovivi and E. Dziaadek, "Omnidirectional antennas for wireless communication," in *Proc. IEEE Int. Symp. on Antennas Propag.*, Jul. 11–16, 1999, vol. 1, pp. 556–559.
- [14] T. Noro and Y. Kazama, "Low profile and wide bandwidth characteristics of top loaded monopole antenna with shorting post," in *Proc. IEEE Int. Workshop on Antenna Technol. Small Antennas and Novel Metamater.*, Mar. 6–8, 2006, pp. 108–111.
- [15] C. Delaveaud, P. Levegue, and B. Jecko, "Small-sized low-profile antenna to replace monopole antennas," *Electron. Lett.*, vol. 34, pp. 716–717, Apr. 1998.
- [16] G. Goubau, "Multielement monopole antennas," in *Proc. Workshop on Electrically Small Antennas ECOM*, Ft. Monmouth, NJ, May 1976, pp. 63–67.
- [17] C. Ravipati and S. Best, "The goubau multi element monopole antenna—Revisited," in *Proc. IEEE Int. Symp. on Antennas Propag.*, Jun. 10–15, 2007, pp. 233–236.
- [18] F. Yang and Y. Rahmat-Samii, "Reflection phase characterizations of the EBG ground plane for low profile wire antenna applications," *IEEE Trans. Antennas Propag.*, vol. 51, pp. 2691–2703, Oct. 2003.
- [19] N. Behdad and K. Sarabandi, "Bandwidth enhancement and further size reduction of a class of miniaturized slot antennas," *IEEE Trans. Antennas Propag.*, vol. 52, pp. 1928–1935, Aug. 2004.



Wonbin Hong (S'05) received the B.S. degree in from Purdue University, West Lafayette, IN, in 2004 and the M.S. degree from the University of Michigan, Ann Arbor, in 2005, all in electrical engineering.

He is currently a Graduate Research Assistant with the Radiation Laboratory, the University of Michigan, while working toward the Ph.D. degree in applied electromagnetics. His research concentration is on efficiency enhancement and miniaturization of printed antennas for integrated systems.



Kamal Sarabandi (S'87–M'90–SM'92–F'00) received the B.S. degree in electrical engineering from the Sharif University of Technology, Tehran, Iran, in 1980, the M.S. degree in electrical engineering in 1986, and the M.S. degree in mathematics and the Ph.D. degree in electrical engineering from The University of Michigan, Ann Arbor, in 1989.

He is the Director of the Radiation Laboratory and a Professor in the Department of Electrical Engineering and Computer Science, University of Michigan. His research areas of interest include

microwave and millimeter-wave radar remote sensing, Meta-materials, electromagnetic wave propagation, and antenna miniaturization. He has 22 years of experience with wave propagation in random media, communication channel modeling, microwave sensors, and radar systems and is leading a large research group including two research scientists, 12 Ph.D. and 2 M.S. students. He has graduated 30 Ph.D. and supervised numerous postdoctoral students. He has served as the Principal Investigator on many projects sponsored by NASA, JPL, ARO, ONR, ARL, NSF, DARPA and a larger number of industries. He has published many book chapters and more than 160 papers in refereed journals on miniaturized and on-chip antennas, metamaterials, electromagnetic scattering, wireless channel modeling, random media modeling, microwave measurement techniques, radar calibration, inverse scattering problems, and microwave sensors. He has also had more than 420 papers and invited presentations in many national and international conferences and symposia on similar subjects.

Dr. Sarabandi is a member of the NASA Advisory Council appointed by the NASA Administrator. He also served as a Vice President of the IEEE Geoscience and Remote Sensing Society (GRSS) and a member of the IEEE Technical Activities Board Awards Committee. He is serving on the Editorial Board of the IEEE PROCEEDINGS, and served as Associate Editor of the IEEE TRANSACTIONS ON ANTENNAS AND PROPAGATION and the *IEEE Sensors Journal*. He is a member of Commissions F and D of URSI and is listed in *American Men & Women of Science*, *Who's Who in America*, and *Who's Who in Science and Engineering*. He was the recipient of the Henry Russel Award from the Regent of The University of Michigan. In 1999 he received a GAAC Distinguished Lecturer Award from the German Federal Ministry for Education, Science, and Technology given to about ten individuals worldwide in all areas of engineering, science, medicine, and law. He was also a recipient of the 1996 EECSS Department Teaching Excellence Award and a 2004 College of Engineering Research Excellence Award. In 2005 he received two prestigious awards, namely, the IEEE GRSS Distinguished Achievement Award and the University of Michigan Faculty Recognition Award. He also received the best paper Award at the 2006 Army Science Conference. In 2008 he was awarded a Humboldt Research Award from The Alexander von Humboldt Foundation of Germany granted to scientists and scholars in all disciplines with internationally recognized academic qualifications. In the past several years, joint papers presented by his students at a number of international symposia (IEEE APS'95,'97,'00,'01,'03,'05,'06,'07; IEEE IGARSS'99,'02,'07; IEEE IMS'01, USNC URSI'04,'05,'06, AMTA'06, URSI GA'08) have received student paper awards.